MATEC Web of Conferences **5**, 04035 (2013)
DOI: 10.1051/matecconf/20130504035

Physico-chemical studies of $MgNa_3P_3O_{10} \cdot 12H_2O$

I. Fahim, M. Tridane and S. Belaaouad[a]

Laboratoire de recherche de chimie-Physique Générale des Matériaux, Faculté des Sciences Ben M'sik, BP. 7955, Casablanca. Morocco

Abstract. A magnesium-sodium triphosphate $MgNa_3P_3O_{10} \cdot 12H_2O$ already known has been prepared by the method of ion exchange resin of aqueous chemistry and studied by X-Ray diffraction, thermal analyses (TGA-DTA), differential scanning calorimetry (DSC) and infrared spectrometry which show the characteristic bands of a triphosphate $P_3O_{10}^{5-}$. The results of differential thermal analysis, X-Ray powder diffraction and IR spectra of the compound heated at different temperatures showed that, after dehydration, $MgNa_3P_3O_{10} \cdot 12H_2O$ decomposes into an amorphous compound, then it crystallizes at 600 °C in order to give the anhydrous triphosphate $MgNa_3P_3O_{10}$. $MgNa_3P_3O_{10}$ is stable until its melting point at 612 °C. Two different methods Ozawa and KAS have been selected in studying the kinetics of thermal behavior of the triphosphate P_3O_{10} for the first time. The kinetic and thermodynamic characteristics of the dehydration of $MgNa_3P_3O_{10} \cdot 12H_2O$ and the thermal phenomena accompanying this dehydration were determinated and discussed on the basis of the proposed crystalline structure.

INTRODUCTION

Mixed bivalent cation alkaline triphosphates have not yet been extensively characterized, and only a few of them have been well characterized and studied by thermal behavior. Up to now, in the bivalent cation-sodium triphosphate field only the triphosphates of the type $M^{II}Na_3P_3O_{10} \cdot 12H_2O$ with M^{II} = bivalent cation = Cu, Ni, Co, Mn, Zn, Cd and Mg have been prepared and characterized crystallographically in the first time by A. Jouini [1]. The X-ray analysis showed that all these salts were isotypic. The crystal structure has been solved with the magnesium-sodium triphosphate $MgNa_3P_3O_{10} \cdot 12H_2O$ [1]. These salts are not stable for a long time. This instability can be explained by the fact that some of the water molecules are of a zeolitic nature [2]. The thermal dehydration of the triphosphates $M^{II}Na_3P_3O_{10} \cdot 12H_2O$ with M^{II} = bivalent cation = Cu, Ni, Co, Mn, Zn, Cd and Mg leads to their anhydrous forms $M^{II}Na_3P_3O_{10}$. This work deals with a chemical preparation, thermal behavior, kinetic and IR studies of the first triphosphate $MgNa_3P_3O_{10} \cdot 12H_2O$. The kinetic of thermal dehydration of $MgNa_3P_3O_{10} \cdot 12H_2O$ was studied using thermal analyses TGA-DTA. In this work, the kinetics and thermodynamic parameters for the dehydration process of $MgNa_3P_3O_{10} \cdot 12H_2O$ are reported for the first time.

MATERIALS AND METHODS

1) Chemical preparation

Polycrystalline samples of the $MgNa_3P_3O_{10} \cdot 12H_2O$ compound, were prepared by adding slowly dilute triphosphoric acid to an aqueous solution of magnesium II carbonate and sodium carbonate, according to the following chemical reaction:

$$H_5P_3O_{10} + MgCO_3 + 3/2Na_2CO_3 + 19/2H_2O \rightarrow MgNa_3P_3O_{10} \cdot 12H_2O + 5/2CO_2.$$

The preliminary obtained solution was then slowly evaporated at room temperature until polycrystalline samples of $MgNa_3P_3O_{10} \cdot 12H_2O$ were obtained. The triphosphoric acid used in this reaction was prepared from an aqueous solution of $Na_5P_3O_{10}$ passed through an ion-exchange resin "Amberlite IR 120". The solution passage rate through the cation exchanger was 2 mL/min [3].

2) Characterisation

2.1) X-ray diffraction

Powder diffraction patterns were registered with an automatic diffractometer Siemens D5000, operating in Bragg-Brentano geometry ($\theta/2\theta$). It is equipped with a cooper anticathode ($\lambda_{K\alpha} = 1.5406$ Å) and a rear monochrome. The footstep of measurement is 0,02° (2θ) for an angular range $10° < 2\theta° < 70°$ for the compound. Integration time for each footstep measurement is 30 s.

2.2) Chemical analyses

The chemical analysis was carried out by microanalysis X with a probe type Kevex implanted on a sweeping electron microscope (MEB).

2.3) Infrared spectrometry

Spectra were recorded in the range 4000–400 cm^{-1} with a Perkin-Elmer IR 983G spectrophotometer, using samples dispersed in spectroscopically pure KBr pellets.

[a] e-mail: belaaouad.s@gmail.com

Table 1. Results of the chemical analyses and dehydration of $MgNa_3P_3O_{10} \cdot 12H_2O$.

	P	Ni	Na	H_2O
Theoretical	3	1	3	12
Experimental	2.999	1	2.999	11.999

2.4) Thermal behavior

Thermal analyses TGA-DTA coupled were performed using the multimodule 92 Setaram Analyzer operating from room temperature up to 800 °C, in a platinum crucible, at various heating rates from 1 to 18 °C.min^{-1}.

Differential scanning calorimetry (DSC) was carried out with a NETZSCH DSC 200PC apparatus.

RESULTS AND DISCUSSION

1) Crystal data

$MgNa_3P_3O_{10} \cdot 12H_2O$ is monoclinic $P2_1/n$ with the following unit-cell dimensions: a = 15.049(1) Å, b = 9.245(4) Å, c = 14.722(3) Å, $\beta = 90.00°$, Z = 4. $MgNa_3P_3O_{10} \cdot 12H_2O$ has never been studied except its crystallographic characterization [1].

The results of the chemical analyses and dehydration of the reaction product are in total accordance with the formula $MgNa_3P_3O_{10} \cdot 12H_2O$ and are summarized in Table 1.

2) Chemical stability

The triphosphate dodecahydrate of nickel-sodium $MgNa_3P_3O_{10} \cdot 12H_2O$, is stable under the conditions of temperature and pressure of our laboratory until 50 °C. We have followed, by IR spectrometry, X-ray diffraction and thermogravimetric analyses, the stability of $MgNa_3P_3O_{10} \cdot 12H_2O$ during six months, and no evolution was observed. After six months and approximately one week $MgNa_3P_3O_{10} \cdot 12H_2O$ is not stable. This instability can be explained by the fact that two of the water molecules are of a zeolitic nature [2]. The X-ray diffraction pattern of $MgNa_3P_3O_{10} \cdot 12H_2O$ is shown in Figure 1.

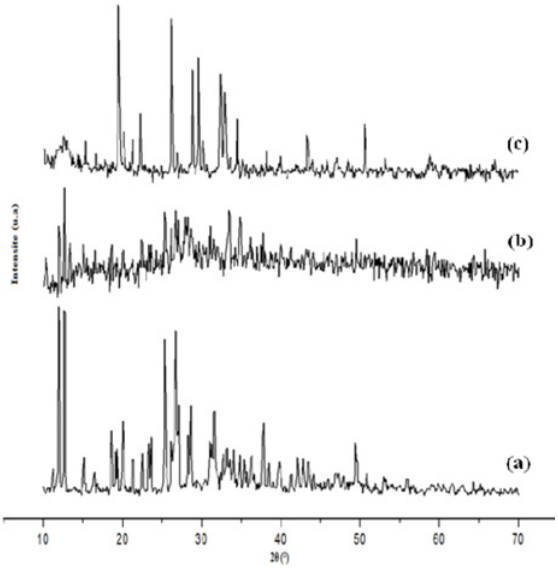

Figure 1. X-ray powder diffractograms of the phosphates (a) $MgNa_3P_3O_{10} \cdot 12H_2O$, (b) evolution to $MgNa_3P_3O_{10}$, (c) $MgNa_3P_3O_{10}$.

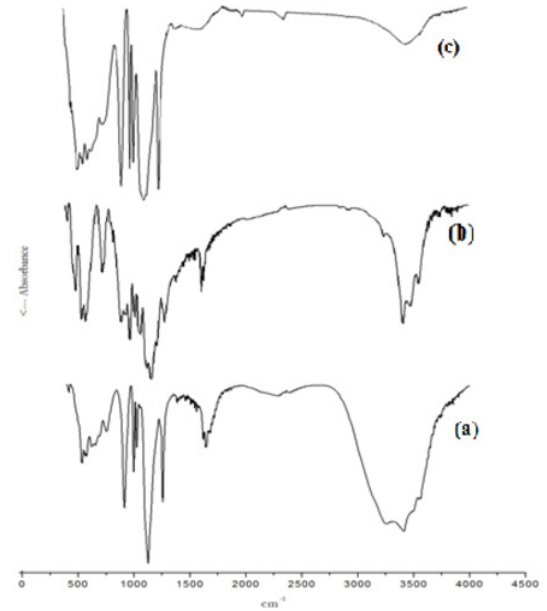

Figure 2. IR spectra of the phosphates (a) $MgNa_3P_3O_{10} \cdot 12H_2O$, (b) evolution to $MgNa_3P_3O_{10}$, (c) $MgNa_3P_3O_{10}$.

3) IR study. Characterization of $MgNa_3P_3O_{10} \cdot 12H_2O$ by IR vibration spectrometry

The infrared spectrum (Figure 2) of a KBr pressed pellet containing the powdered sample of $MgNa_3P_3O_{10} \cdot 12H_2O$ was studied in the range 4000–400 cm^{-1} using a Perkin-Elmer IR 983G spectrophotometer. Band assignments for the fundamental modes, of valence and bending, of $P_3O_{10}^{5-}$ anions are presented in Table 2. The frequencies of the $P_3O_{10}^{5-}$ anion are assigned on the basis of the characteristic vibrations of the P–O–P bridge [4,5], PO_2 and PO_3 groups. As the P–O bond in the PO_2 and PO_3 group is weaker than that in the P–O–P bridge, the vibrational frequencies of PO_2 and PO_3 are expected to be higher than those for P–O–P. The bands due to the symmetric and antisymmetric-stretching frequencies of PO_2 and PO_3 in $P_3O_{10}^{5-}$ are generally observed in the region 1190–1010 cm^{-1} [4,5]. The bands observed in the domain 970–840 cm^{-1} are attributed to the antisymmetric and symmetric POP stretching modes. The bands due to δ(OPO), $\delta(PO_2)$, $\delta(PO_3)$ and δ(POP) are also identified in Table 2.

The obtained frequencies for the $P_3O_{10}^{5-}$ ion are comparable with those observed in the infrared spectra of $MNa_3P_3O_{10} \cdot 12H_2O$ (M= Cu, Co, Ni, Mn) [5–7].

Table 2. Characterization of $MgNa_3P_3O_{10} \cdot 12H_2O$ by IR vibration spectrometry.

$\nu_{observed}$, (cm^{-1})	movement [5]
3460	ν O-H
1688	ν_δ HOH
1291	ν P = O
1266	ν_{as} PO_2
1160	ν_{as} PO_3
1034	ν_s PO_2
998	ν_s PO_3
905	ν_{as} POP
753	ν_{as} POP
687	ν_s POP
654	ν_s POP
575	δ PO_2
529	δ PO_3
417	δPOP

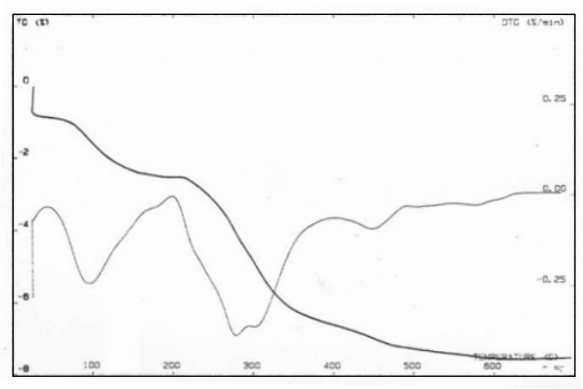

Figure 3. TGA (TG-DTG) curves of $MgNa_3P_3O_{10} \cdot 12H_2O$ at rising temperature (6 °C min^1).

Table 3. Characterization of $MgNa_3P_3O_{10}$ by IR vibration spectrometry.

$\nu_{observed}$, (cm^{-1})	movement [5]
1338	νP=O
1252	ν_{as} PO_2
1132	ν_{as} PO_3
1029	ν_s PO_2
989	ν_s PO_2
908	ν_s PO_3
755	ν_{as} POP
664	ν_s POP
616	ν_s POP
570	δ PO_2
528	δ PO_3
468	δ POP

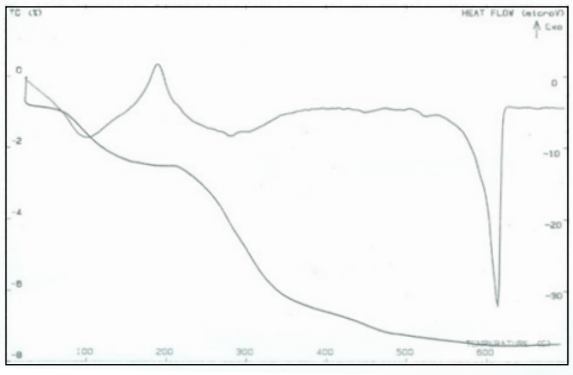

Figure 4. DTA curve of $MgNa_3P_3O_{10} \cdot 12H_2O$ at rising temperature (6 ° $C.min^{-1}$).

4) Thermal behavior

Non isothermal study [8,9]. The two curves corresponding to the TG and DTG analyses in air atmosphere and at a heating rate 6 °C.min^{-1} of $MgNa_3P_3O_{10} \cdot 12H_2O$ are given in Figure 3.

The dehydration of the triphosphate dodecahydrate of magnesium-sodium $MgNa_3P_3O_{10} \cdot 12H_2O$ occurs in three steps in three temperature ranges 81–213 °C, 213–345 °C and 345–578 °C (Figure 3). In the thermo gravimetric (TG) curve (Figure 3),

The first stage between 81 and 213 °C corresponds to the elimination of 3 water molecules, the second stage from 213 to 345 °C is due to the elimination of 6 water molecules and the third stage 345–578 °C corresponds to the elimination of 3 water molecules.

The derivative of the TG curve, DTG, of $MgNa_3P_3O_{10} \cdot 12H_2O$ under atmospheric pressure and at a heating rate 6 ° C min^{-1} Figure 3 contains three peaks due to the dehydration of $MgNa_3P_3O_{10} \cdot 12H_2O$. The first very intensive peak in the domain 44–164 °C, observed at 99 ° C is due to the departure of 3 water molecules. The second intensive peak in the range 200–362 °C, appears as a doubled, situated at 275 and 264 °C is due to the evolving of 6 water molecules. The third step are located between 400 and 488 °C, it occurs at about 451 °C, and it corresponds to the departure of three water molecules.

Figure 4, showing the differential thermal analysis (DTA) curve of $MgNa_3P_3O_{10} \cdot 12H_2O$ under atmospheric pressure and at a heating rate 6 °C.min^{-1}, reveals 3 effects. The first endothermic peak, well pronounced at 100 °C is due to the removal of water molecules in the title compound. The second exothermic peak is well pronounced at 191 °C and corresponds to the formation of the anhydrous triphosphate $MgNa_3P_3O_{10}$ [10]. The last peak is rather related to the melting point of $MgNa_3P_3O_{10}$ at 612 °C.

5) Step manner study

The thermal behavior of $MgNa_3P_3O_{10} \cdot 12H_2O$ was also studied in a step manner of temperature by X-ray diffraction and IR absorption spectrometry between 25 and 600 °C. X-ray diffraction patterns recorded after annealing for 36 hours at different temperatures reveal that $MgNa_3P_3O_{10} \cdot 12H_2O$ is stable up to 50 °C (Figures 1 and 2).

The removal of three water molecules of hydration of $MgNa_3P_3O_{10} \cdot 12H_2O$, observed in the temperature range 81–213 °C, destroyed the crystalline network and brings to an intermediate amorphous phase [11] which does not diffract the X-ray (Figure 1), nor exhibits the IR absorption bands characteristic of a triphosphate $P_3O_{10}^{5-}$ (Figure 2).

Table 4. Characteristic temperatures at maximum dehydration rates, T_m in °C, at different heating rates from the DTA curves of $MgNa_3P_3O_{10} \cdot 12H_2O$.

Heating rate v	1 (°C/min)	3 (°C/min)	6 (°C/min)	18 (°C/min)
First peak	357	372	381	407
Second peak	531	542	582	643
Third peak	713	724	765	851

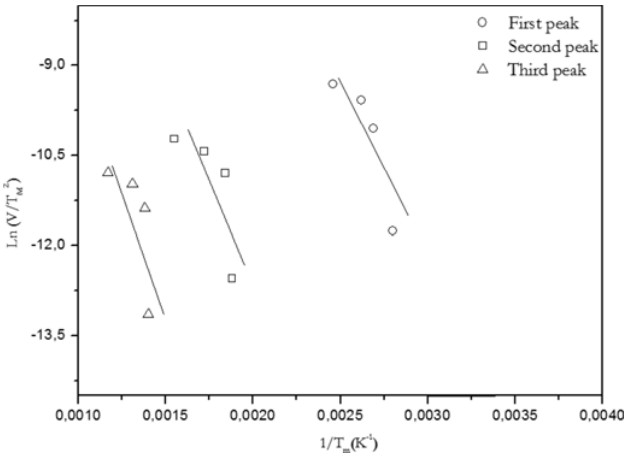

Figure 5. $Ln(v/T_m^2) = f(1/T_m)$ representation of the dehydration thermal effect of the triphosphate $MgNa_3P_3O_{10} \cdot 12H_2O$.

Still six water molecules were removed between 213 and 345 °C and three more were removed between 345 and 578 °C. Between 500 and 600 °C, the obtained X-Ray diffractograms and IR spectra, reveal the crystallization of a phase which is nothing other than the anhydrous form of the triphosphate $MgNa_3P_3O_{10} \cdot 12H_2O$. So, the final product resulting from the dehydration of $MgNa_3P_3O_{10} \cdot 12H_2O$ between 500 and 600 °C is the anhydrous triphosphate $MgNa_3P_3O_{10}$. So, The results of differential thermal analysis (DTA), X- Ray powder diffraction (RX) and IR spectra (IR) of the compound $MgNa_3P_3O_{10} \cdot 12H_2O$ heated at different temperatures showed that, after dehydration, $MgNa_3P_3O_{10} \cdot 12H_2O$ decomposes into an amorphous compound, then it crystallizes at 600 °C in order to give the anhydrous triphosphate $MgNa_3P_3O_{10}$. The IR bands, of valence and bending, observed in the IR spectrum of $MgNa_3P_3O_{10}$ are gathered in Table 4. The IR spectra reveal that the transformation from monoclinic dodecahydrate $MgNa_3P_3O_{10} \cdot 12H_2O$ to its anhydrous form takes place without any strong modification of the symmetry of the $P_3O_{10}^{5-}$ anions [5]. $MgNa_3P_3O_{10}$ is stable until its melting point at 612 °C.

6) Estimation of the thermodynamic functions

Various equations of kinetic analyses are known such as Kissinger's method [12], Kissinger-Akahira-Sunose (KAS) [13], Ozawa [14], Coats-Redfern [15] and Van Krevelen et al. [15] methods. Especially, the Ozawa and KAS equations were well described and widely used in the literature, therefore, these methods are selected in studying the kinetics of thermal dehydration of the $MgNa_3P_3O_{10} \cdot 12H_2O$ compound. So, water loss kinetic parameters were

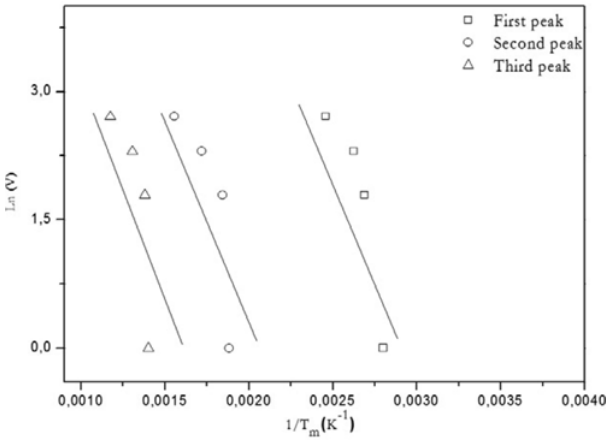

Figure 6. $Ln(v) = f(1/T_m)$ representation of the dehydration thermal effect of the triphosphate $MgNa_3P_3O_{10} \cdot 12H_2O$.

evaluated using the Kissinger-Akahira-Sunose (KAS) [13] and Ozawa [14] methods, from the curves $ln(v/T_m^2) = f(1/T_m)$ and $ln(v) = f(1/T_m)$ (Figures 5 and 6), where v is the heating rate and T_m the sample temperature at the thermal effect maximum. The characteristic temperatures at maximum dehydration rates, T_m, for the triphosphate $MgNa_3P_3O_{10} \cdot 12H_2O$ are shown in Table 5.

From these temperature and according to the Kissinger – Akahira – Sunose (KAS) [13] and Ozawa [14] methods, the apparent activation energies of dehydration were calculated for the triphosphate $MgNa_3P_3O_{10} \cdot 12H_2O$ (Table 6). For the Kissinger – Akahira – Sunose (KAS) [13] method, the slope of the resulting straight line of the curve : $ln(v/T_m^2) = f(1/T_m)$ (Figure 5), equals to $-E_a/R$, allows the apparent activation energy to be calculated (Table 6). Concerning the Ozawa [14] method, the slope of the resulting straight line on the curve : $ln(v) = f(1/T_m)$ (Figure 6), equals to $-1.0516E/R$, allows also the apparent activation energy (Table 6) to be calculated by this second way. The equations used for the two methods are the following:

For KAS [13]

$$\ln\left(\frac{v}{T_m^2}\right) = \ln\left(\frac{AR}{E}\right) - \left(\frac{E}{R}\right)\left(\frac{1}{T_m}\right). \quad (1)$$

For OZAWA [15]

$$\ln v = \ln\left(\frac{AR}{1.0516E}\right) - 1.0516\left(\frac{E}{R}\right)\left(\frac{1}{T_m}\right). \quad (2)$$

The pre-exponential factor or Arrhenius constant (A) can be calculated from both KAS [14] and Ozawa [14] methods. The related thermodynamic functions can be calculated by using the activated complex theory (transition state) of Eyring [17–19]. The following general equation can be written: [20]

$$A = \left(\frac{e\chi k_B T_m}{h}\right)\exp\left(\frac{\Delta S^*}{R}\right) \quad (3)$$

where e is the Neper number (e = 2.7183), χ is the transition factor, which is unity for the monomolecular reaction, k_B is the Boltzmann constant ($k_B = 1.3806 \times$

Table 5. Activation energy values E_a, pre-exponential factor (A) and correlation coefficient (r^2) calculated by Ozawa and KAS methods for the dehydration of $MgNa_3P_3O_{10} \cdot 12H_2O$ under atmospheric pressure.

Model	Ozawa Method			KAS Method		
	E_a (kJ.mol^{-1})	r^2	$A(10^{+14}\,\mathrm{min}^{-1})$	E_a (kJ.mol^{-1})	r^2	$A\ (10^{+4}\,\mathrm{min}^{-1})$
First peak	59.137	0.8093	9.3793	55.840	0.8723	78008
Second peak	8268	0.8679	1.2086	45.122	0.8493	7.2382
Third peak	52163	0.8142	3.5031	62.788	0.8492	8.8813

Table 6. Values of ΔS^*, ΔH^* and ΔG^* for dehydration step of $MgNa_3P_3O_{10} \cdot 12H_2O$ calculated according to Ozawa and KAS equations.

Model	Ozawa Method			KAS Method		
	ΔS^*(kJ.mol^{-1}.K^{-1})	ΔH^*(kJ.mol^{-1})	ΔG^*(kJ.mol^{-1})	ΔS^*(kJ.mol^{-1}.K^{-1})	ΔH^*(kJ.mol^{-1})	ΔG^*(kJ.mol^{-1})
First peak	−0.0249	56.043	56.968	−0.1911	52.746	96.987
Second peak	−0.0227	28264	28.276	−0.1992	40.615	14.861
Third peak	−0.0163	52157	52.159	−0.1999	56.768	20.153

10^{-23} J.K^{-1}), h is Plank's constant (h=6.6261×10^{-34} J.s), T_m is the peak temperature of the DTA curve, R is the gas constant (R = 8.314 J.K^{-1}.mol^{-1}) and ΔS^* is the entropy change of transition state complex or entropy of activation. Thus, the entropy of activation may be calculated as follows:

$$\Delta S^* = R \ln\left(\frac{Ah}{e_\chi k_B T_m}\right). \quad (4)$$

The enthalpy change of transition state complex or heat of activation (ΔH^*) and Gibbs free energy of activation (ΔG^*) of decomposition were calculated according to Eqs. (5) and (6), respectively:

$$\Delta H^* = E^* - RT_m \quad (5)$$

$$\Delta G^* = \Delta H^* - \Delta S^* T_m. \quad (6)$$

Where, E^* is the activation energy E_a of both KAS [14] and Ozawa [15] methods. The values of the activation energy are gathered in Table 6. Thermodynamic functions were calculated from Eqs. (4), (5) and (6) and summarized in Table 7. The negative values of ΔS^* from two methods for the dehydration step reveals that the activated state is less disordered compared to the initial state. These ΔS^* values suggest a large number of degrees of freedom due to rotation which may be interpreted as a «slow» stage [20,21] in this step. The positive values of ΔG^* at all studied methods are due to the fact that, the dehydration processes are not spontaneous.

The positivity of ΔG^* is controlled by a small activation entropy and a large positive activation enthalpy according to the Eq. 6. The endothermic peaks in DTA data agree well with the positive sign of the activation enthalpy (ΔH^*). The estimated thermodynamic functions ΔS^* and ΔG^* (Table 7) from two methods are different to some extent due to the different pre-exponential factor of about 10^{10} as in the case of $CuNa_3P_3O_{10} \cdot 12H_2O$ [5]. While ΔH^* (Table 7) exhibits an independent behavior on the pre-exponential factor as seen from exhibiting nearly the same value.

CONCLUSION

The present work concerns the preparation and the dehydration of $MgNa_3P_3O_{10} \cdot 12H_2O$. This study allows us the identification of final product of dehydration, $MgNa_3P_3O_{10}$, a new phase. This anhydrous triphosphate which is stable until its melting point at 612°C was characterized crystallography. The passage from the dodecahydrated phase, $MgNa_3P_3O_{10} \cdot 12H_2O$ monoclinic, to the anhydrous one, $MgNa_3P_3O_{10}$ hexagonal system, occurs with the passage by an amorphous phase. Water molecules of $MgNa_3P_3O_{10} \cdot 12H_2O$ which are of constitution, remove the solid in three kinetic steps with activation energies of dehydration calculated by Ozawa and KAS methods. In fact, in this work, the kinetic and thermodynamic parameters for the dehydration process of $MgNa_3P_3O_{10} \cdot 12H_2O$ have been calculated and reported for the first time. We have examinated and interpreted the IR spectra, in the domain 400–4000 cm^{-1}, of the $MgNa_3P_3O_{10} \cdot 12H_2O$ compound and its anhydrous form $MgNa_3P_3O_{10}$.

The thermal behavior of $MgNa_3P_3O_{10} \cdot 12H_2O$ can be summarized by the following schema:

$MgNa_3P_3O_{10} \cdot 12H_2O$
↓81-213 °C
Amorphous phase + $3H_2O$
↓213-345 °C

Amorphous phase + $6H_2O$
↓345-578 °C
$MgNa_3P_3O_{10}$ + $3H_2O$
↓612 °C
Melting of $MgNa_3P_3O_{10}$

References

[1] A. Jouini, Thèse d'état, Monastir, Tunisie (1988).
[2] A. Durif, *Cry. Chem. Cond. Phos.,* (Plenum Press, New York (1995).
[3] A. Jouini, A. Durif, *C.R. Acad. Sci.,* 297-II, 573 (1983).
[4] D.E.C. Corbridge, E.J. Lowe, *J. Chem. Soc.,* 493 (1954).

[5] A. Charaf, I. Fahim, EL.M. Tace, M. Tridane, M. Radid, S. Belaaouad., *Pho. Rese. Bull*., 24, 83 (2010).
[6] K. Azzaoui, R. Essehli, E. Mejdoubi, B. El Bali, M. Dusek, K. Fejfarova., *Int. J. Inor. Chem.,* 702, 471 (2012).
[7] V. I. Popova, V. A. Popov, E. V. Sokolova, G. Ferraris, N. V. Chukanov., *N. Jb. Miner. Mh*., *Jg*, 3, 117 (2002).
[8] B. V. L'vov, Thermal Decomposition of Solids and Melts. *Hot Topics in Thermal Analysis and Calorimetry*, 7, 33 (2007).
[9] B. V. L'vov, Thermal Decomposition of Solids and Melts. *Hot Topics in Thermal Analysis and Calorimetry*, 7, 65 (2007).
[10] I. Fahim, A. Kheireddine, M. Tridane, S. Belaaouad., *Powd. Diffr.,* 26, 78 (2011).
[11] J. R. V. Wazer, K. A. Holst, *J. Amer. Chem. Soc.,* 72, 639 (1950).
[12] H. E. Kissinger, *Anal. Chem.,* 29, 1702 (1957).
[13] T. Akihira, T. Sunose, *Res. Report Chiba Inst. Technol.,* 16, 22 (1971).
[14] T. Ozawa, *Chem. Soc. Jpn.,* 38, 1881 (1965).
[15] W. Coats, J. P. Redfern, *Nature,* 68, 201 (1964).
[16] D.W. Van Krevelns, P. J. Hoftijzer, *Trans. Inst. Chem. Eng.,* 32, 5360 (1954).
[17] D. Young, Decomposition of solides, Academia Prague (1984).
[18] J. Rooney, *J. Molec. Catal. A. Chem.,* L1, 96 (1995).
[19] B. Boonchom, *J. Chem. Eng. Data.,* 53, 1533 (2008).
[20] L. Vlaev, N. Nedelchev, K. Gyurova, M. Zagorcheva, *J. Anal. Appl. Pyrol.,* 81, 253 (2008).
[21] P. Noisong, C. Danavirutai, T. Boonchom., *Sol. Stat. Sci.,* 10, 1598 (2008).